Electronic Supplementary Material (ESI) for Physical Chemistry Chemical Physics.

Supporting Information

Structural and thermodynamic study of Ca A- or Co B-site substituted $SrFeO_{3-\delta}$ perovskites for low temperature chemical looping applications

Giancarlo Luongo, Felix Donat and Christop R. Müller*

Laboratory of Energy Science and Engineering, Department of Mechanical and Process Engineering
ETH Zürich, Leonhardstrasse 21, 8092 Zürich, Switzerland

*Corresponding author

(muelchri@ethz.ch Prof. Christoph Müller)

1. Characterisation of the oxygen carriers

Crystal structure

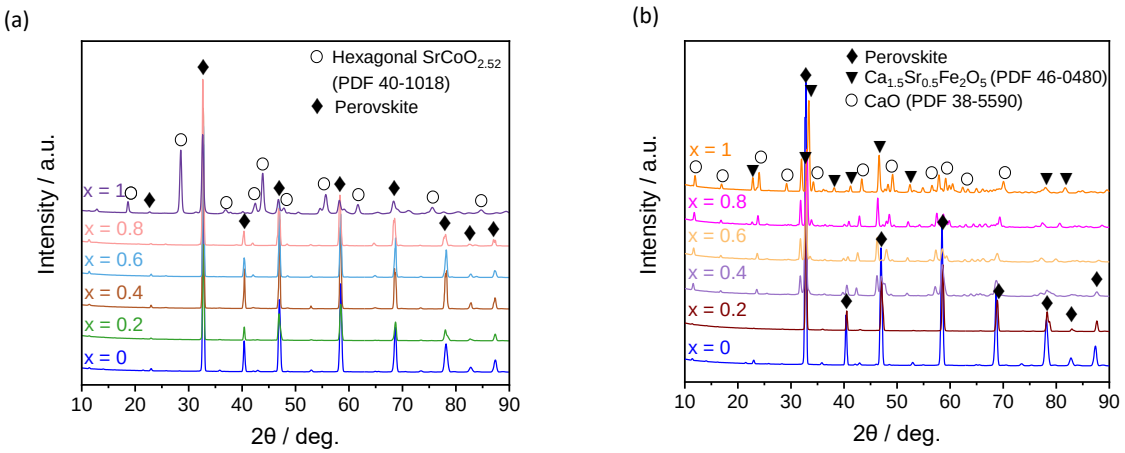

Figure S1 – Synchrotron based XRD patterns of the prepared (a) $SrFe_{1-x}Co_xO_{3-\delta}$ (x = 0, 0.2, 0.4, 0.6, 0.8, 1) and (b) $Sr_{1-x}Ca_xFeO_{3-\delta}$ (x = 0, 0.2, 0.4, 0.6, 0.8, 1) collected at the ID31 beamline of the European Synchrotron Radiation Facility (ESRF). The XRD data were collected using a wavelength of λ = 0.1770 Å (ID31, ESRF) in transmission geometry. The patterns were transformed to λ = 1.5405 Å to compare with the laboratory XRD patterns.

Composition: ICP-OES results

Table S1 – ICP-OES results of the investigated phase-pure perovskites with composition $SrFe_{1-x}Co_xO_{3-\delta}$ (x = 0, 0.2, 0.4, 0.6, 0.8, 1) and $Sr_{1-x}Ca_xFeO_{3-\delta}$ (x = 0.1, 0.2, 0.25).

Nominal composition	Elemental chemical composition (atom%)				Composition, as per ICP-OES analysis
	Ca	Co	Fe	Sr	
$SrFeO_{3-\delta}$	-	-	-	-	$Sr_{0.99}Fe_{1.01}O_{3-\delta}$
$SrFe_{0.8}Co_{0.2}O_{3-\delta}$	-	3.80	16.20	20.00	$SrFe_{0.81}Co_{0.19}O_{3-\delta}$
$SrFe_{0.6}Co_{0.4}O_{3-\delta}$	-	8.00	12.00	20.00	$SrFe_{0.6}Co_{0.4}O_{3-\delta}$
$SrFe_{0.4}Co_{0.6}O_{3-\delta}$	-	12.01	8.00	20.01	$SrFe_{0.4}Co_{0.6}O_{3-\delta}$
$SrFe_{0.2}Co_{0.8}O_{3-\delta}$	-	4.20	15.80	20.00	$SrFe_{0.21}Co_{0.79}O_{3-\delta}$
$Sr_{0.9}Ca_{0.1}FeO_{3-\delta}$	2.00	-	20.00	18.00	$Sr_{0.9}Ca_{0.1}FeO_{3-\delta}$
$Sr_{0.8}Ca_{0.2}FeO_{3-\delta}$	4.10	-	20.00	15.90	$Sr_{0.8}Ca_{0.20}FeO_{3-\delta}$
$Sr_{0.75}Ca_{0.25}FeO_{3-\delta}$	5.20	-	20.00	14.80	$Sr_{0.74}Ca_{0.26}FeO_{3-\delta}$

Thermogravimetric analysis

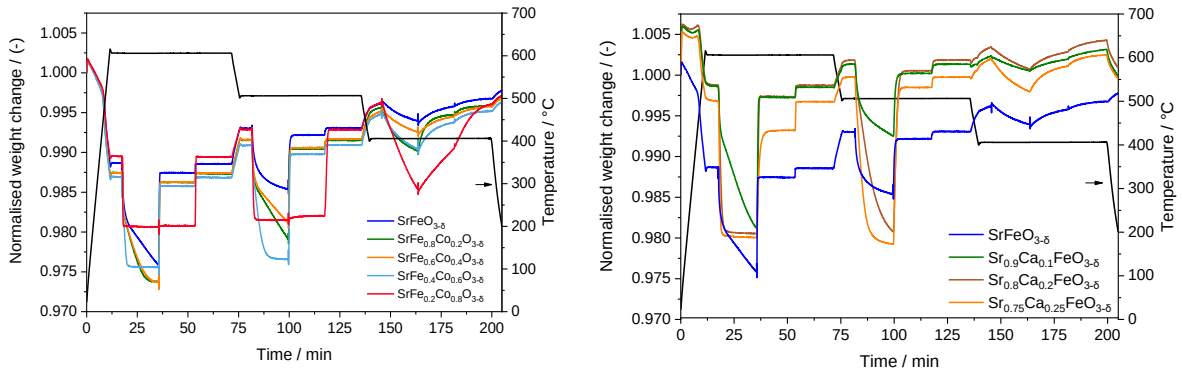

Figure S2 – Thermogravimetric measurements performed on the perovskites with composition $SrFe_{1-x}Co_xO_{3-\delta}$ (x = 0, 0.2, 0.4, 0.6, 0.8, 1) and $Sr_{1-x}Ca_xFeO_{3-\delta}$ (x = 0.1, 0.2, 0.25).

2. Oxygen desorption properties

Cyclic redox stability

(a) (b)

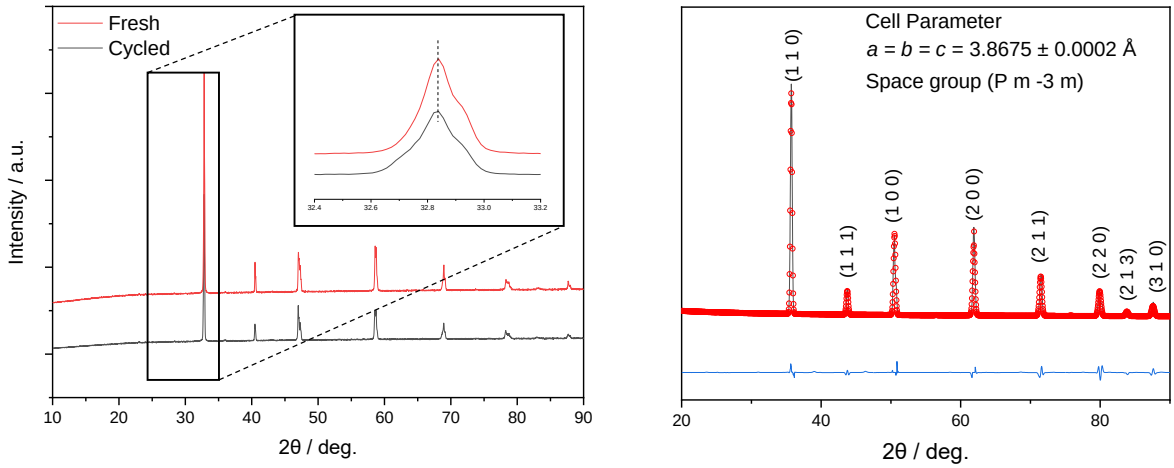

Figure S3 – (a) XRD patterns of the perovskite with composition $Sr_{0.8}Ca_{0.2}FeO_{3-\delta}$ before and after 30 redox cycles in the TGA at 500°C and (b) full pattern Rietveld refinement of the cycled sample.

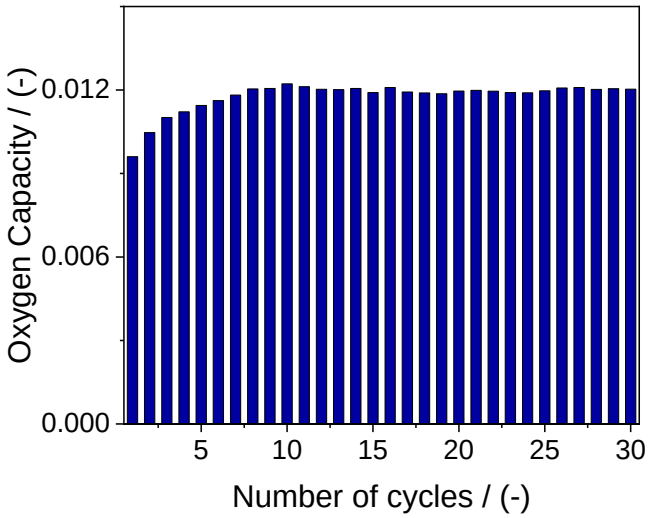

Figure S4 – Oxygen capacity as a function of cycle number, measured in the TGA using the sample $SrFe_{0.2}Co_{0.8}O_{3-\delta}$ at 500 °C, corresponding to 30 redox cycles (reduction in pure N_2, oxidation in air).

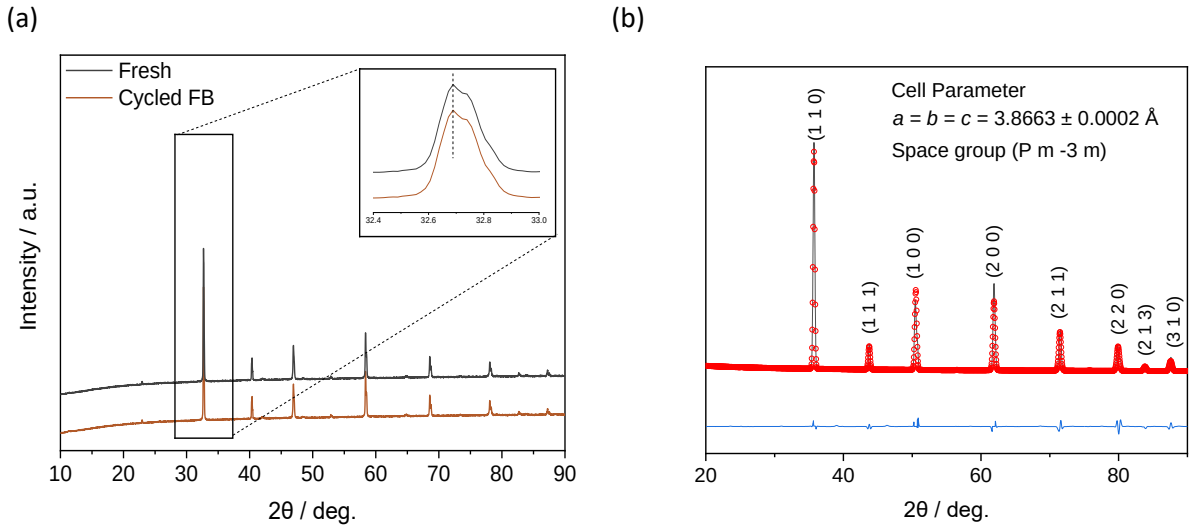

Figure S5 – (a) XRD patterns of the perovskite with composition $SrFe_{0.2}Co_{0.8}FeO_{3-\delta}$ before and after 30 redox cycles in the TGA at 500°C and (b) full pattern Rietveld refinement of the cycled sample.

Table S2 – Textural characteristics of the oxygen carriers, before and after redox cycling experiments: BET surface area, BJH pore volume

Sample	Surface area [$m^2\ g^{-1}$]	Pore volume [$cm^3\ g^{-1}$]
$SrFe_{0.2}Co_{0.8}O_{3-\delta}$ before cycling	0.96	0.001
$SrFe_{0.2}Co_{0.8}O_{3-\delta}$ after cycling	1.15	0.003
$Sr_{0.8}Ca_{0.2}FeO_{3-\delta}$ before cycling	1.87	0.002
$Sr_{0.8}Ca_{0.2}FeO_{3-\delta}$ after cycling	1.95	0.0025

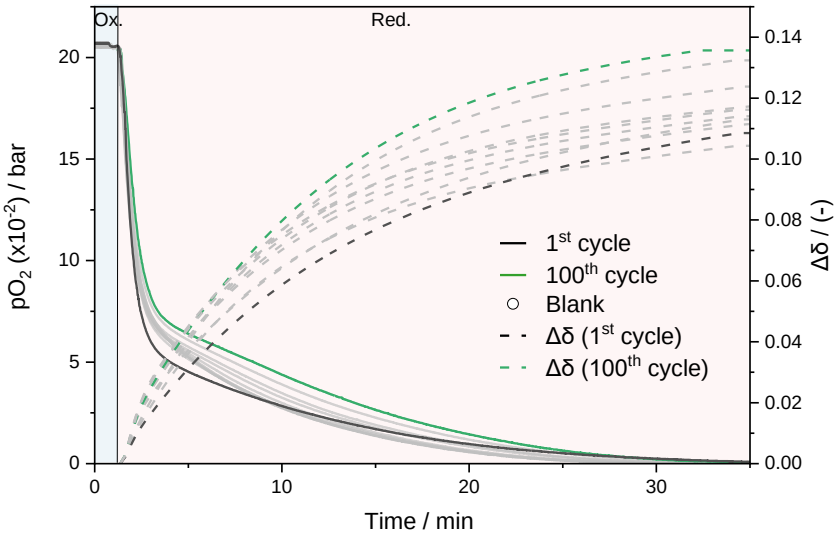

Figure S6 – pO_2 measured at the outlet of the fixed bed reactor for cycle 1 (black) and cycle 100 (green) with respective evolution of $\Delta\delta$ (dashed lines) for the material with composition $SrFe_{0.2}Co_{0.8}O_{3-\delta}$ at T = 500 °C and 50 mL min^{-1} flow of N_2. The grey lines represent measurements for every cycle up to number 10.

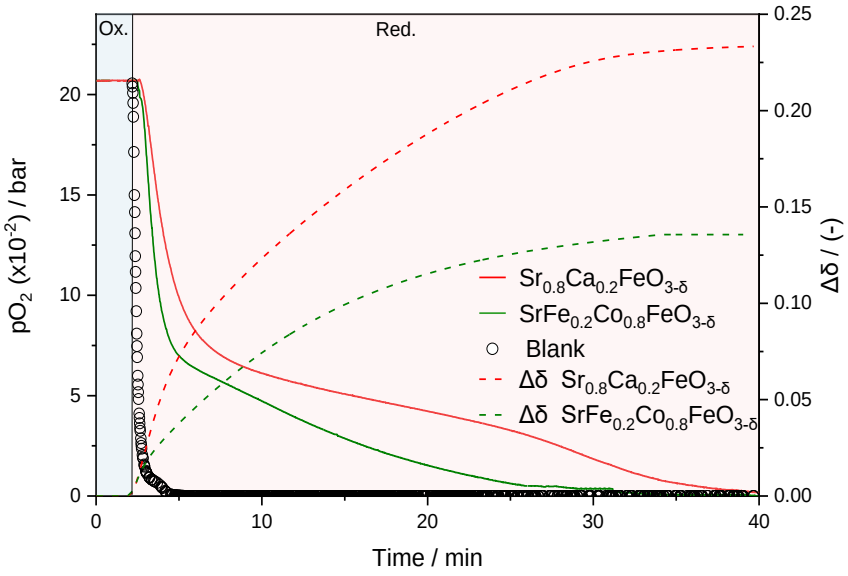

Figure S7 – Comparison of the pO_2 measured at the outlet of the fixed bed reactor for cycle 100 of $Sr_{0.8}Ca_{0.2}FeO_{3-\delta}$ (red) and $SrFe_{0.2}Co_{0.8}O_{3-\delta}$ (green) with respective evolution of $\Delta\delta$ (dashed lines) at T = 600 °C and 50 mL min^{-1} flow of N_2.

3. Thermodynamic assessment

Initial oxygen non-stoichiometry

Table S3 – Results of the iodometric titration for the calculation of the initial oxygen non-stoichiometry at ambient T and p.

Sample	$3-\delta_0$
$SrFeO_{3-\delta}$	2.78
$SrFe_{0.8}Co_{0.2}O_{3-\delta}$	2.77
$SrFe_{0.6}Co_{0.4}O_{3-\delta}$	2.76
$SrFe_{0.4}Co_{0.6}O_{3-\delta}$	2.78
$SrFe_{0.2}Co_{0.8}O_{3-\delta}$	2.68
$Sr_{0.9}Ca_{0.1}FeO_{3-\delta}$	2.84
$Sr_{0.8}Ca_{0.2}FeO_{3-\delta}$	2.85
$Sr_{0.75}Ca_{0.25}FeO_{3-\delta}$	2.84

HP-TG thermogravimetric measurement of $SrFe_{1-x}Co_xO_{3-\delta}$

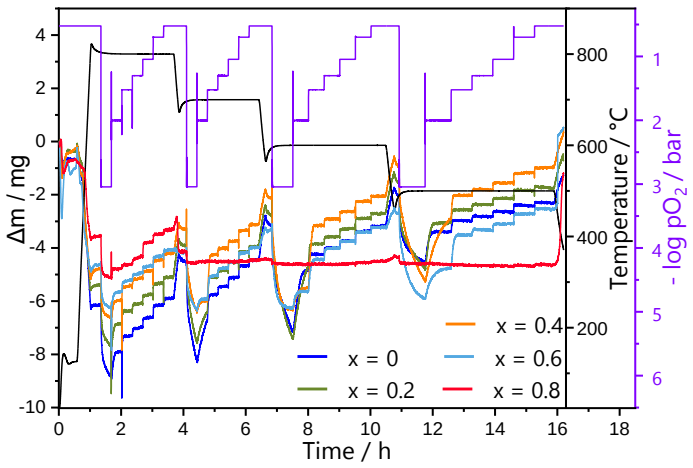

Figure S8 Sample weight change as a function of time, *T* and pO_2 for the samples with composition $SrFe_{1-x}Co_xO_{3-\delta}$ (x = 0, 0.2, 0.4, 0.6, 0.8).

Phase diagrams for $SrFe_{1-x}Co_xO_{3-\delta}$

(a)

(b)

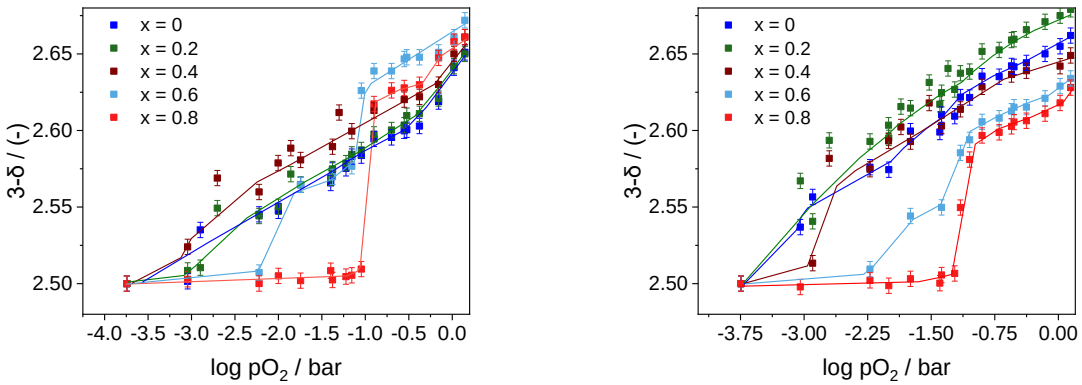

(c)

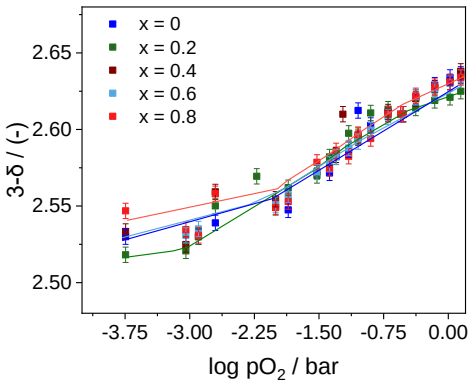

Figure S9 – Measured oxygen non-stoichiometry (symbols) as a function of pO_2 for the samples with composition $SrFe_{1-x}Co_xO_{3-\delta}$ (x = 0, 0.2, 0.4, 0.6, 0.8) at (a) 600 °C, (b) 700 °C and (c) 800 °C.

HP-TG thermogravimetric measurement

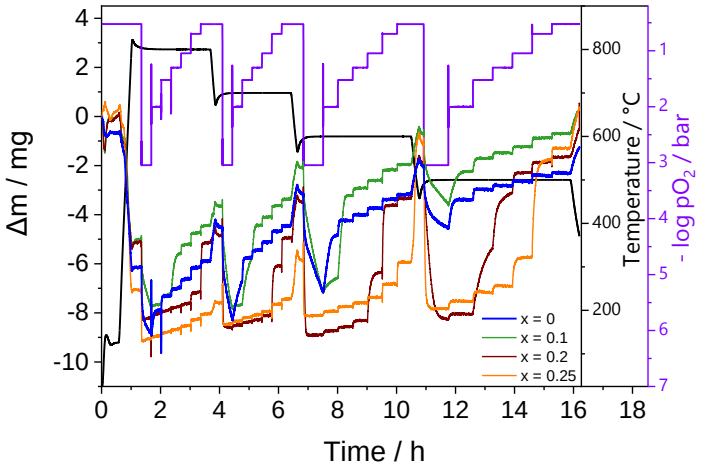

Figure S10 – Sample weight change as a function of time, T and pO_2 for the samples with composition $Sr_{1-x}Ca_xFeO_{3-\delta}$ (x = 0.1, 0.2, 0.25).

Phase diagrams for $Sr_{1-x}Ca_xFeO_{3-\delta}$

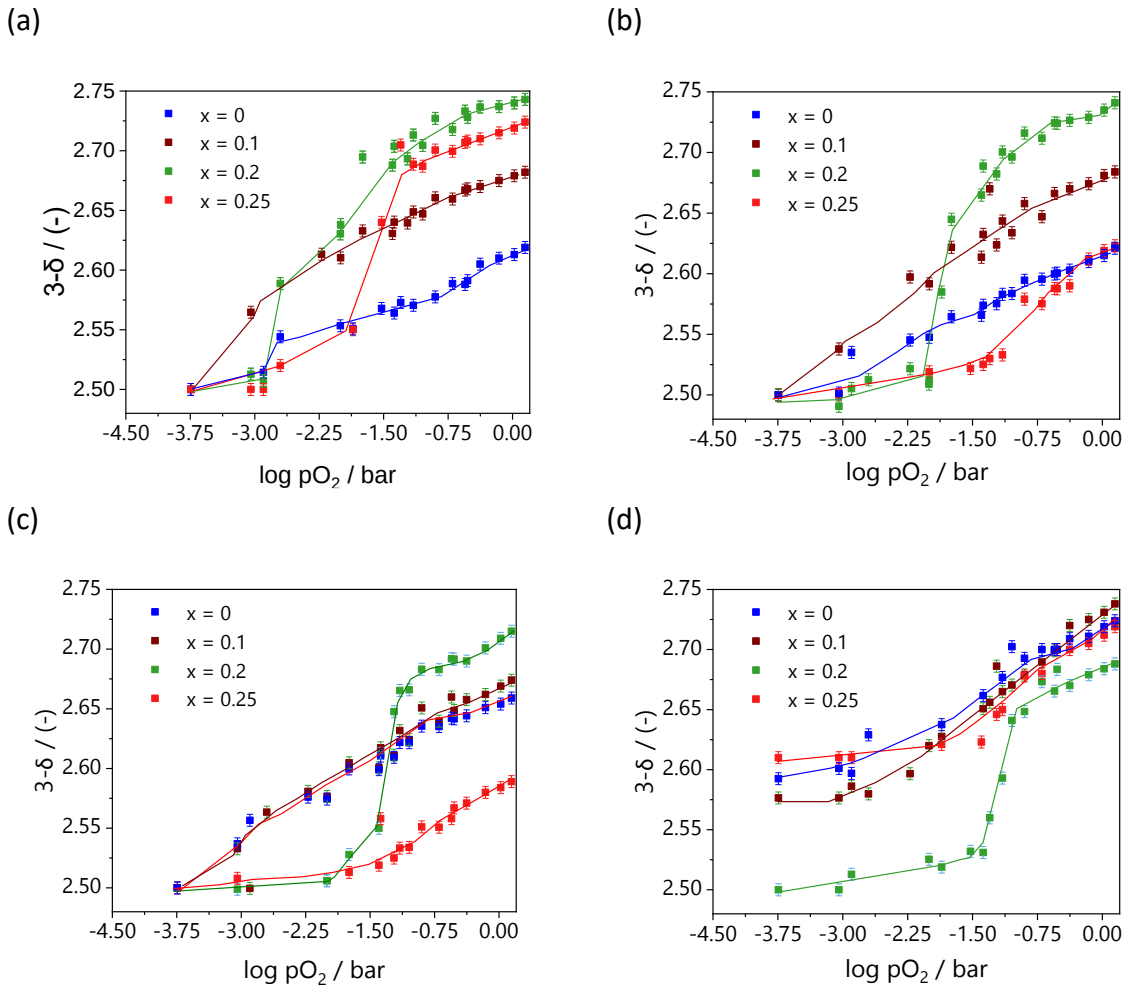

Figure S11 – Measured oxygen non-stoichiometry (symbols) as a function of pO_2 for the samples with composition $Sr_{1-x}Ca_xFeO_{3-\delta}$ (x = 0, 0.1, 0.2, 0.25) at (a) 500 °C, (b) 600 °C, (c) 700 °C and (d) 800 °C.

Arrhenius plots for $SrFe_{1-x}Co_xO_{3-\delta}$

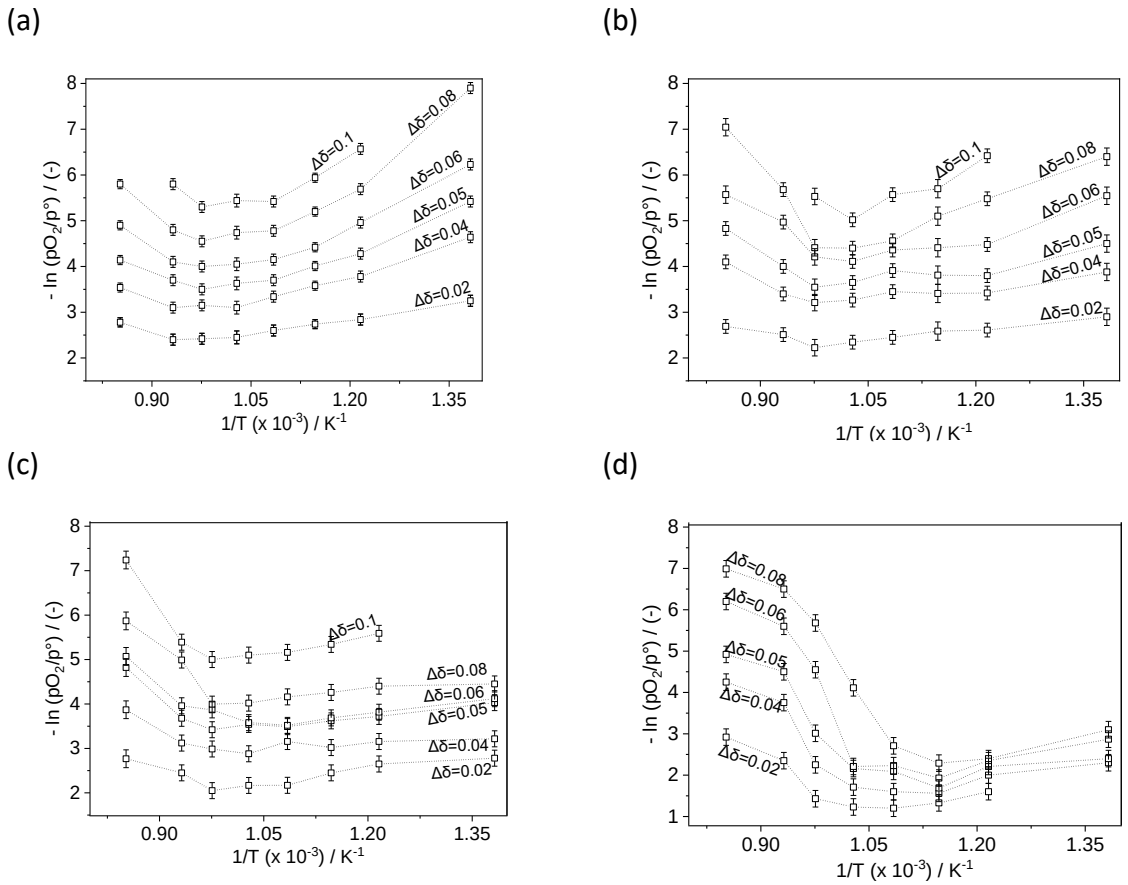

Figure S12 - Arrhenius plots for (a) $SrFeO_{3-\delta}$, (b) $SrFe_{0.6}Co_{0.4}O_{3-\delta}$, (c) $SrFe_{0.4}Co_{0.6}O_{3-\delta}$ and (d) $SrFe_{0.2}Co_{0.8}O_{3-\delta}$

Arrhenius plots for $Sr_{1-x}Ca_xFeO_{3-\delta}$

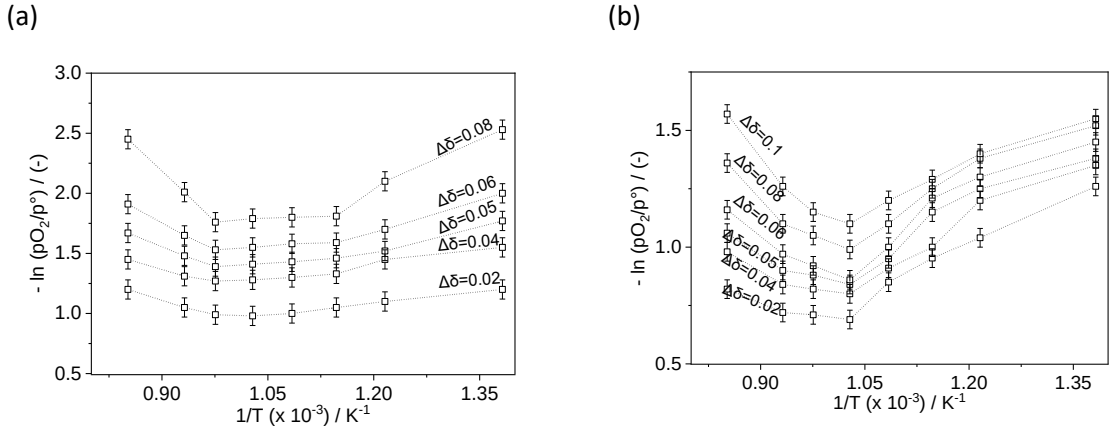

Figure S13 - Arrhenius plots for (a) $Sr_{0.9}Ca_{0.1}FeO_{3-\delta}$ and (c) $Sr_{0.75}Ca_{0.25}FeO_{3-\delta}$

Enthalpy and entropy of formation for $Sr_{1-x}Ca_xFeO_{3-\delta}$

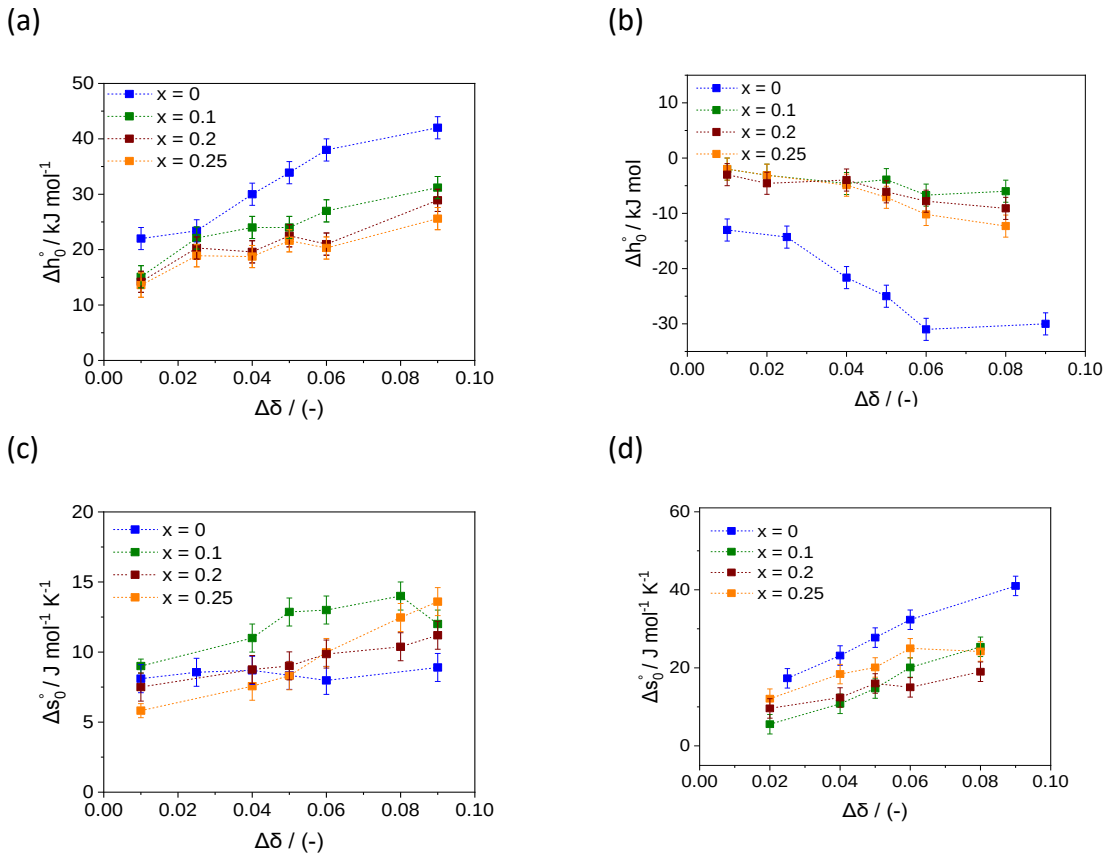

Figure S14 – Evolution of partial molar enthalpy and entropy of formation of vacancies as a function of oxygen non-stoichiometry δ in the (a, b) high temperature regime (T > ~770 °C), and (c, d) low temperature (T < ~770 °C) respectively, for $Sr_{1-x}Ca_xFeO_{3-\delta}$.

Table S4 – Partial molar enthalpy and entropy of vacancy formation of the investigated samples. The values after ± indicate the 95% confidence intervals.

Temperature < 770 °C						
Δδ	$SrFeO_{3-\delta}$		$SrFe_{0.8}Co_{0.2}O_{3-\delta}$		$SrFe_{0.6}Co_{0.4}O_{3-\delta}$	
	$\Delta h_0°$ [kJ mol]	$\Delta s_0°$ [J mol^{-1} K^{-1}]	$\Delta h_0°$ [kJ mol]	$\Delta s_0°$ [J mol^{-1} K^{-1}]	$\Delta h_0°$ [kJ mol]	$\Delta s_0°$ [J mol^{-1} K^{-1}]
0.01	22.1±0.84	8.1±0.7	19±1.92	5±0.5	14.5±1.3	6±0.5
0.025	23.4±0.97	8.55±0.72	20.1±1.9	5.4±0.5	13.6±1.2	7.02±0.53
0.04	30.1±1.17	8.7±0.75	23.8±1	6.15±0.8	18.6±1.4	9.75±0.9
0.05	33.8±1.51	8.3±0.71	28.7±1.6	6.26±0.95	22.9±1.78	11.45±1.06
0.06	38.2±1.22	8±0.7	30.4±1.9	6.45±1.2	28±1.2	12.2±1.17
0.09	42.3±1	8.9±0.77	37±1.5	7.34±0.77	28.9±1.32	12.82±1.27

Temperature > 770 °C						
Δδ	$SrFeO_{3-\delta}$		$SrFe_{0.8}Co_{0.2}O_{3-\delta}$		$SrFe_{0.6}Co_{0.4}O_{3-\delta}$	
	$\Delta h_0°$ [kJ mol]	$\Delta s_0°$ [J mol^{-1} K^{-1}]	$\Delta h_0°$ [kJ mol]	$\Delta s_0°$ [J mol^{-1} K^{-1}]	$\Delta h_0°$ [kJ mol]	$\Delta s_0°$ [J mol^{-1} K^{-1}]
0.01	-13±0.97		-13.23±1.4		-5.1±1.02	
0.025	-14.3±1.17	17.3±1.1	-11.1±1.24	18.9±1.1	-7.5±1.78	21.6±1.1
0.04	-21.6±1.51	23.15±1.1	-17.2±1.05	26.88±1.1	-8.9±1.54	32.4±1.1
0.05	-25.1±1.22	27.74±1.5	-19.05±1.74	34.9±1.5	-10.4±1.6	44.29±1.5
0.06	-31.05±1	32.33±1.45	-25.2±1.6	40.9±1.45	-7.6±1.25	53.19±1.45
0.09	-30.1±1.2	53.5±1.36	-22.3±1.53	46.3±1.36	-9.1±1.55	64.27±1.36

	Temperature < 770 °C					
Δδ	$SrFe_{0.4}Co_{0.6}O_{3-\delta}$		$SrFe_{0.2}Co_{0.8}O_{3-\delta}$		$Sr_{0.9}Ca_{0.1}FeO_{3-\delta}$	
	$\Delta h_0°$ [kJ mol]	$\Delta s_0°$ [J mol^{-1} K^{-1}]	$\Delta h_0°$ [kJ mol]	$\Delta s_0°$ [J mol^{-1} K^{-1}]	$\Delta h_0°$ [kJ mol]	$\Delta s_0°$ [J mol^{-1} K^{-1}]
0.01	10±2	7±1.2	8±1.2	3±1.2	10.8±0.37	5.87±1.13
0.025	11.8±1.91	6.3±1.65	11.8±1.91	2.9±1.65	12.2±0.69	7.56±1.15
0.04	15±1.5	8.13±1.38	10±1.5	3.06±1.38	14.6±0.54	8.31±1.26
0.05	17.7±1.6	9.18±1.	11.29±1.6	3.35±1	16.9±0.87	9.97±1.18
0.06	19.8±1.54	9.28±1.2	12.3±1.54	4.3±1.2	19.7±1.1	12.4±1.1
0.09	23±1.54	11.57±1.05	18.6±1.91	6.78±1.05		

	Temperature > 770 °C					
Δδ	$SrFe_{0.4}Co_{0.6}O_{3-\delta}$		$SrFe_{0.2}Co_{0.8}O_{3-\delta}$		$Sr_{0.9}Ca_{0.1}FeO_{3-\delta}$	
	$\Delta h_0°$ [kJ mol]	$\Delta s_0°$ [J mol^{-1} K^{-1}]	$\Delta h_0°$ [kJ mol]	$\Delta s_0°$ [J mol^{-1} K^{-1}]	$\Delta h_0°$ [kJ mol]	$\Delta s_0°$ [J mol^{-1} K^{-1}]
0.01	-0.5±0.94	27.45±1.24	-0.86±0.88	36.6±1.74	1.19±0.65	5.55±1.1
0.025	-0.59±1.15	50.6±1.54	-0.9±1.24	50.8±1.55	1.57±0.98	10.8±1.34
0.04	-0.52±1.35	64.6±1.44	-2.87±1.35	60.5±1.35	1.93±1.2	14.7±1.32
0.05	-0.51±1.42	64.2±1.32	-2.8±1.21	70.79±1.43	2.43±1.06	20.1±1.1
0.06	-1.01±0.97	81.13±1.3	-2.78±1.1	80.1±1.4	4.18±1.1	25.4±1

	Temperature < 770 °C			
Δδ	$Sr_{0.8}Ca_{0.2}FeO_{3-\delta}$		$Sr_{0.75}Ca_{0.25}FeO_{3-\delta}$	
	$\Delta h_0°$ [kJ mol]	$\Delta s_0°$ [kJ mol]	$\Delta h_0°$ [kJ mol]	$\Delta s_0°$ [J mol^{-1} K^{-1}]
0.01	11.1±0.98	2.18±1.35	10.6±0.75	8.16±1.48
0.025	13.6±1.12	3.14±1.45	14.1±0.56	9.86±1.44
0.04	15.7±1.15	3.54±1.6	17.6±0.96	12.85±1.39
0.05	19.4±1.2	4.65±1.58	25.6±1.02	15.95±1.25
0.06	21.1±1.1	5.02±1.41	28.1±0.87	24.63±1.65
0.09				

	Temperature > 770 °C			
Δδ	$Sr_{0.8}Ca_{0.2}FeO_{3-\delta}$		$Sr_{0.75}Ca_{0.25}FeO_{3-\delta}$	
	$\Delta h_0°$ [kJ mol]	$\Delta s_0°$ [kJ mol]	$\Delta h_0°$ [kJ mol]	$\Delta s_0°$ [J mol^{-1} K^{-1}]
0.01	-4.56±0.68	9.6±1.35	-3.1±0.89	12.1±1.56
0.025	-3.97±0.96	12.4±1.22	-4.9±0.96	18.4±1.85
0.04	-6.1±0.93	16.2±1.46	-7.1±0.87	20.1±1.9
0.05	-7.8±0.78	15±1.54	-10.2±0.88	25±1.85
0.06	-9.1±1	19.1±1.5	-12.3±1.4	24.2±1.7

4. *In-situ* XRD results

(a) T = 600 °C, $SrFeO_{3-\delta}$

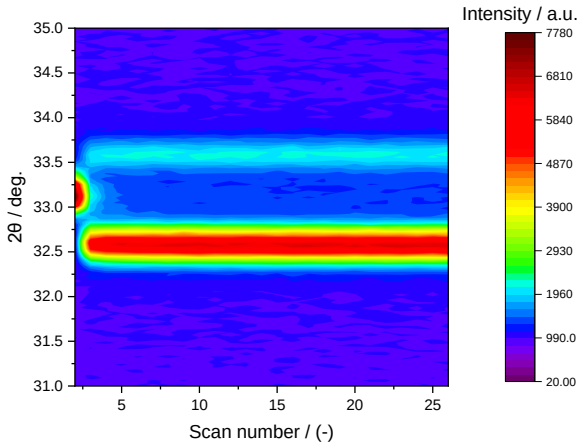

(b) T = 900 °C, $SrFeO_{3-\delta}$

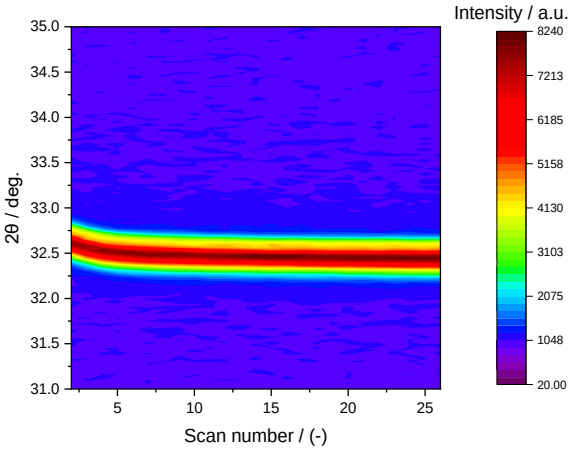

(c) T = 600 °C, $SrFe_{0.6}Co_{0.4}O_{3-\delta}$

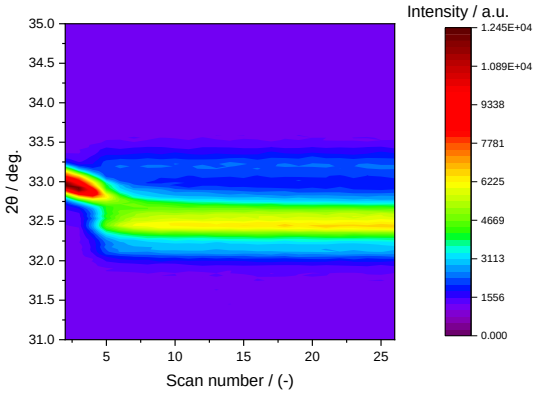

(d) T = 900 °C, $SrFe_{0.6}Co_{0.4}O_{3-\delta}$

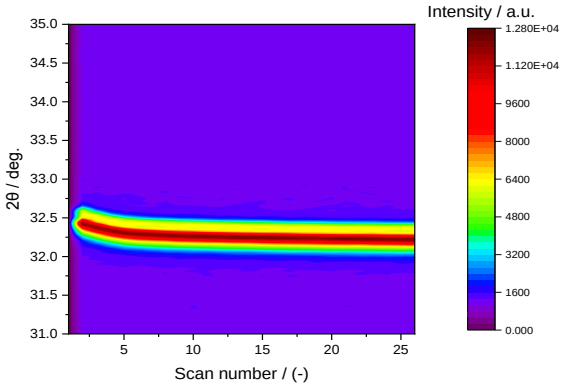

(e) T = 600 °C, $SrFe_{0.4}Co_{0.6}O_{3-\delta}$

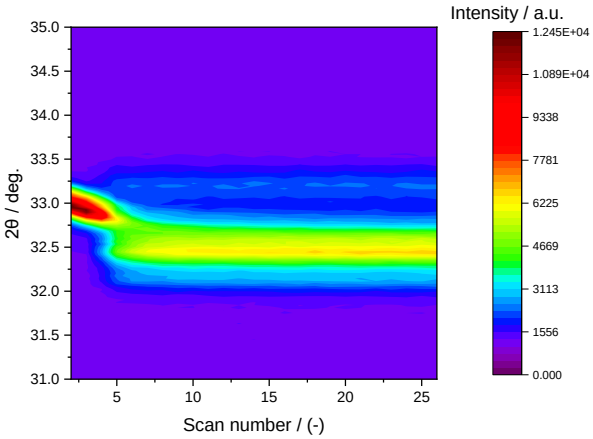

(f) T = 900 °C, $SrFe_{0.4}Co_{0.6}O_{3-\delta}$

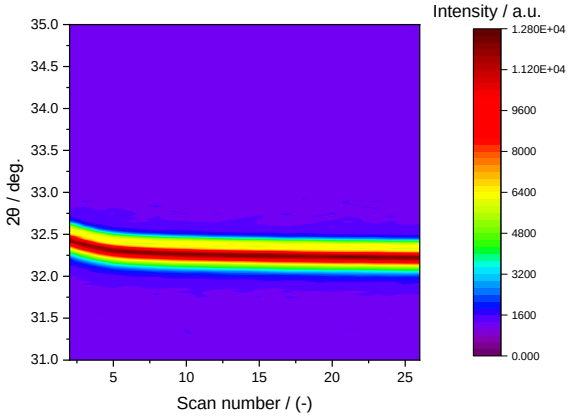

(g) T = 600 °C, $SrFe_{0.2}Co_{0.8}O_{3-\delta}$

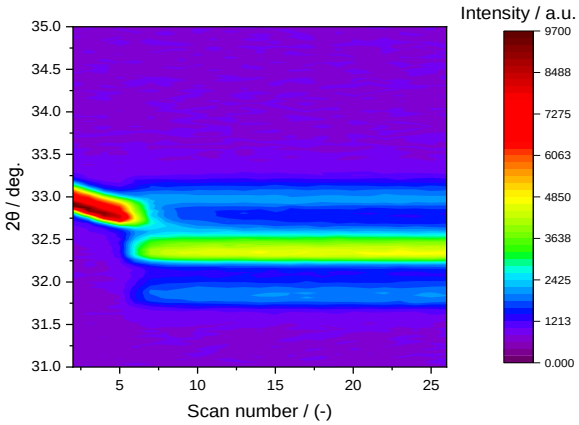

(h) T = 900 °C, $SrFe_{0.2}Co_{0.8}O_{3-\delta}$

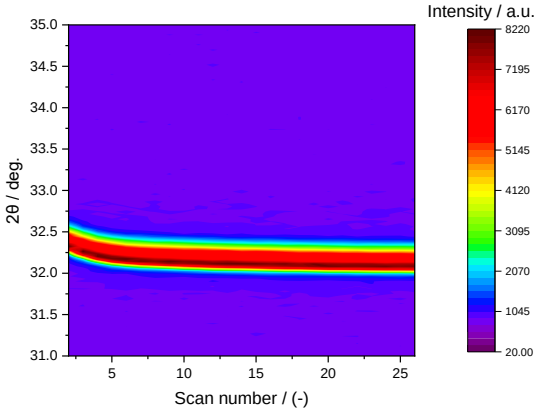

(i) T = 600 °C, $Sr_{0.9}Ca_{0.1}FeO_{3-\delta}$

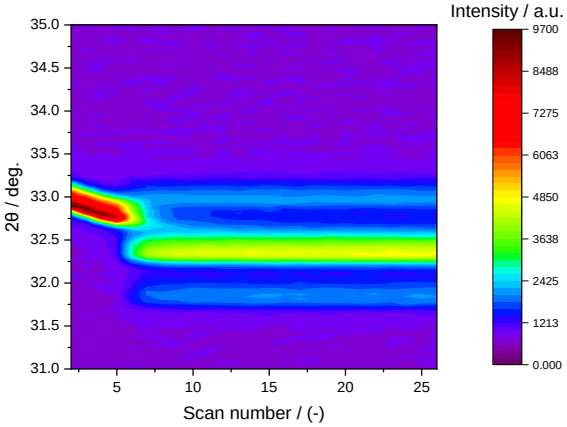

(j) T = 900 °C, $Sr_{0.9}Ca_{0.1}FeO_{3-\delta}$

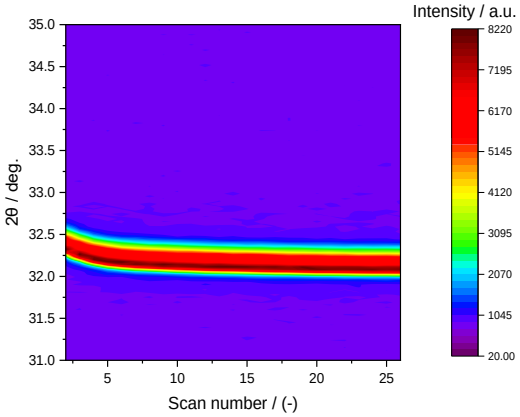

(k) T = 600 °C, $Sr_{0.75}Ca_{0.25}FeO_{3-\delta}$

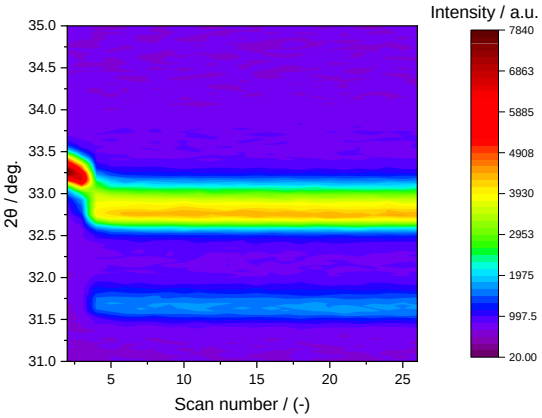

(l) T = 900 °C, $Sr_{0.75}Ca_{0.25}FeO_{3-\delta}$

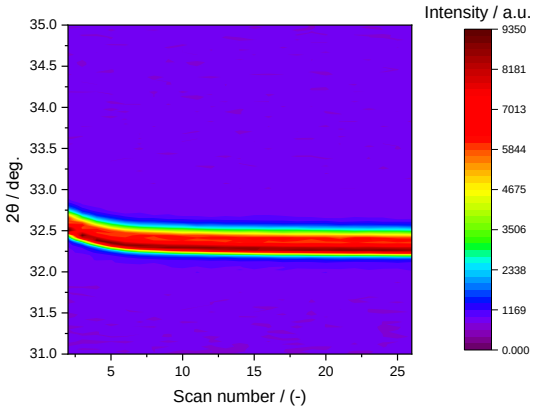

Figure S15 – *In-situ* XRD patterns of $SrFe_{1-x}Co_xO_{3-\delta}$ (x = 0, 0.4, 0.6, 0.8) and $Sr_{1-x}Ca_xFeO_{3-\delta}$ (x = 0.1, 0.25) at T = 600 °C and T = 900 °C, when switching the gas atmosphere from air (pO_2 = $2.09 \cdot 10^{-1}$ bar) to pure N_2 (pO_2 = $7.09 \cdot 10^{-5}$ bar) after scan number 2.